Optics Communications 283 (2010) 1581–1584

Contents lists available at ScienceDirect

Optics Communications

journal homepage: www.elsevier.com/locate/optcom

Invited paper

All-optical active components for dielectric-loaded plasmonic waveguides

A.V. Krasavin *, A.V. Zayats

Centre for Nanostructured Media, IRCEP, The Queen's University of Belfast, Belfast BT7 1NN, UK

ARTICLE INFO

Article history:
Received 3 August 2009
Received in revised form 18 August 2009
Accepted 24 August 2009

Keywords:
Plasmon
Waveguide
Active

ABSTRACT

Dielectric-loaded surface plasmon polariton waveguides (DLSPPWs) provide a very efficient means to localize and guide optical signal, which makes them a promising candidate for the construction of highly-integrated photonic circuits. Here, we present full 3D numerical modelling of highly efficient and compact all-optical active DLSPPW components to achieve a fully functioning active photonic circuit.

1. Introduction

Surface plasmon polaritons have proved to be very efficient in localizing and guiding of photonic signal on a scale which is hardly reachable with conventional dielectric waveguides. This makes them a prospective candidate for downsizing integrated optical circuits. A surface plasmon polariton is an electromagnetic wave coherently coupled to electron oscillations and propagating in a wave-like fashion along a metal–dielectric interface [1]. A large variety of SPP waveguides, based on different geometries and physical principles have been developed [2–7]. One prospective type of the waveguide is the dielectric-loaded surface plasmon polariton waveguide (DLSPPW) formed by a dielectric stripe on the metal surface [8–10] (Fig. 1). The advantage of DLSPPWs compared to other SPP waveguide types is that a dielectric ridge can be easily functionalized to provide thermo-optical, electro-optical, or all-optical functionalities and can be used for the development of active plasmonic components. Moreover, DLSPPWs fabrication is compatible with current lithography process used in the fabrication of electronic circuits. Combined with intrinsic possibility to control optical signals by electronic ones and visa versa, DLSPPWs can lead to the realization of hybrid electro-optical devices.

In a DLSPPW, the plasmonic mode is localized on a scale of several hundreds of nanometers (Fig. 1b). Moreover, the level of photonic integration achievable with DLSPPWs lies in the micrometer scale. The waveguides can be placed with a separation as small as 2–3 μm without any noticeable cross-talk, while the main passive elements, such as bends and splitters have the dimensions of just several micrometers [8]. This leads to the implementation of efficient passive photonic circuit on a basis of DLSPPWs, which has been demonstrated both theoretically and experimentally [8,9]. However, to construct a fully functioning active photonic circuit, allowing not only signal guiding and multiplexing, but signal processing, one inevitably needs to add active plasmonic components to the system. At this step one will encounter the problem: naturally available non-linear materials provide rather small refractive index changes. Here, we addressed this problem by designing compact and efficient active elements, benefiting from various physical effects. Using finite element method (FEM) simulations we demonstrate DLSPPW-based active Waveguide Ring Resonator (WRR) and active Bragg Reflector (BR).

We performed full three-dimensional FEM numerical simulations of a DLSPP waveguide based on a polymer ($n_1 = 1.493$, e.g. PMMA-based) stripe with a crossection $600 \times 600\ nm^2$ on a surface of gold film ($n_2 = 0.55–11.5i$, taken from [11]). As a first step we solved an eigenmode problem in the waveguide geometry and found that at the telecom wavelength range $\lambda = 1500–1620$ nm the waveguide is singlemode for SPP waves, supporting only a fundamental TM_{00} SPP mode. Then we supplied the obtained mode profile as a source of boundary condition in 3D simulations. The validity of 3D simulations has been proved: the mode remains localized within the waveguide and propagating without any radiation losses essentially with the same propagation characteristics (effective refractive index $n_{eff} = 1.25$, propagation length, defined by Ohmic losses $L_{prop} = 42.5$ μm) as in the eigenmode simulation.

2. Waveguide ring resonator

One of the approaches for creating wavelength selective DLSPPW components is a waveguide ring resonator (WRR, Fig. 1c). It is produced by placing a waveguide loop in the vicinity

* Corresponding author.
E-mail address: a.krasavin@qub.ac.uk (A.V. Krasavin).

0030-4018/$ - see front matter © 2009 Elsevier B.V. All rights reserved.
doi:10.1016/j.optcom.2009.08.054

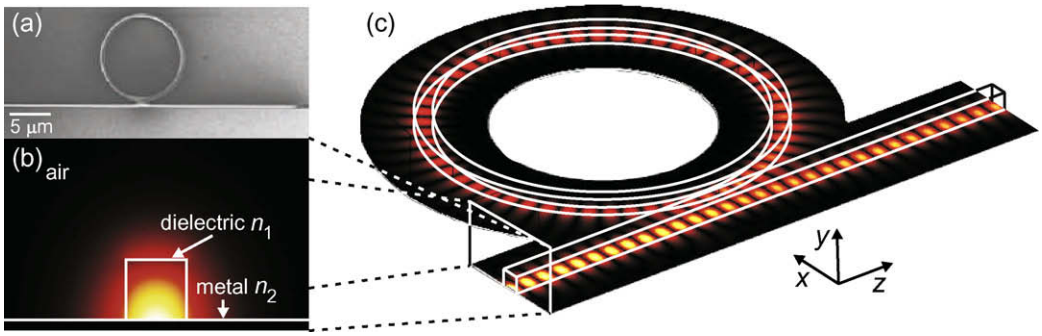

Fig. 1. (a) SEM image of the DLSPP Waveguide Ring Resonator fabricated by deep ultraviolet lithography [12]. (b) Crossection of 600 × 600 nm DLSPP waveguide and abs(E_y) field profile of a fundamental TM_{00} SPP mode in it. (c) Full 3D FEM numerical simulation of ring resonator, the field map represents the absolute value of the electric field component perpendicular to the metal *abs*(E_y) at the metal surface.

of a straight DLSPP waveguide. It has been proven both theoretically and experimentally that WRR is a highly efficient passive element for wavelength selection [12]. Due to the coupling between two nearby waveguides [8,13], some of the input mode S_0 propagates further in the straight waveguide, but some L_0 is transferred to the ring (see inset to Fig. 2b). Once the mode L_0 has completed one round trip in the ring, the inverse process happens. Part S_1 of the ring mode is coupled back into the straight section, interfering with S_0 and the rest L_1 continues to propagate in the ring interfering with the initial ring mode. The same redistribution happens after each cycle: $L_1 \rightarrow S_2 + L_2, \ldots$. Although the interference in the output waveguide and in the ring is quite complicated ([14, p. 198]), involving many partial waves with different amplitude and phase relations, the final outcome is bounded between two extreme scenarios. The first is when the wave initially passed through S_0 and the sum of all the waves decoupled from the ring $\Sigma = S_1 + S_2 + \ldots$ are out of phase. In this case the transmission is minimum. The other output happens when the optical path of the mode in the ring is half a wavelength longer or shorter, then the S_0 and Σ are in phase and the transmission is maximum. An alternative point of view which leads to the same result is to consider superposition of SPP mode circulating in the ring as a ring resonator mode, though highly coupled to the straight waveguide (see for example [14, p. 188, 15]).

The wavelength at which the SPP transmission experiences one or the other outcome mainly depends on the ring radius, since it defines the optical path and consequently all the phase relations. The contrast in the transmission, however, mainly depends on the gap between the ring and the straight section, since it defines the coupling strength and consequently all the amplitudes of the interfering waves. Here we carefully adjusted the gap size so that in the case of the minimum transmission, not only S_0 and Σ were out of phase, but also they have equal magnitudes. Thus we obtained zero minimum transmission (Fig. 2a). Depending on the phase gained by the mode propagating around the ring, the outcome is obviously dependant on the wavelength. While scanning through wavelength a sharp transmission resonance is observed: wavelength difference between full and zero transmission can be as small as 15 nm. Note that the ring radius sufficient for such good wavelength selectivity is just ~5.5 μm, corresponding to the device size of just ~11 μm.

Looking at the WRR from another prospective, it is clear that this device is particularly suitable as the basis for an active element. In this context it is the phase gain acquired by an SPP mode in the ring which is important. At a fixed ring radius and fixed gap between the waveguides it depends on the effective refractive index of the mode in the ring, which in turn is defined by the refractive index of the material. This leads to the idea of fabricating the ring from non-linear optical material, the optical properties of which can be changed by external stimulation, and through this modulate the transmission of an SPP wave.

We adjust the radius of the WRR so that at the desirable wavelength $\lambda = 1548$ nm the slope of the transmission curve is highest, consequently the change in the refractive index will give the big-

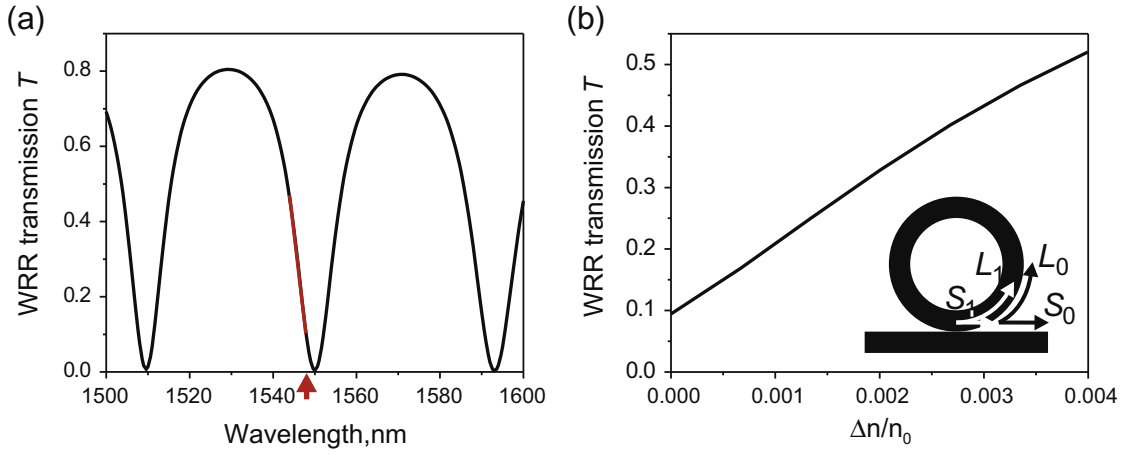

Fig. 2. (a) FEM numerical simulation of the wavelength-selective transmission of the SPP mode through WRR with radius $R = 5.508$ μm and center-to-center distance between the waveguides $d = 159$ nm. The red line shows the region with the steepest slope in transmission, while the red arrow shows the choice of the operation wavelength for the active device. (b) Active WRR element: transmission as a function of the refractive index change in the ring material. Inset shows redistribution of SPP partial waves. (For interpretation of the references to colours in this figure legend, the reader is referred to the web version of this paper.)

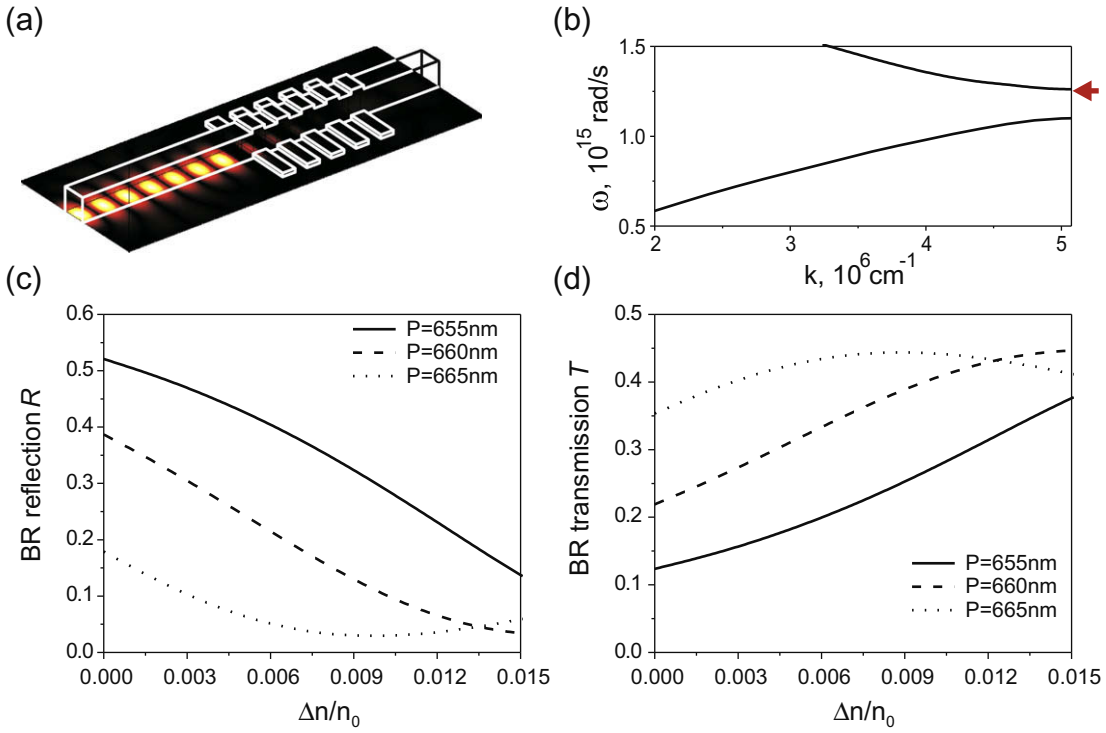

Fig. 3. (a) Active Bragg reflector based on a rectangular metallic grating placed on the surface of metal. Field map presents the absolute value of the electric field component perpendicular to the metal $abs(E_y)$ at the metal surface. (b) Dispersion characteristics of the mode on the BR grating for the case of the frequency being close to the bandgap (the frequency is indicated by the red arrow). (c) Simulated reflection from and (d) transmission through the Bragg reflector with 10 grating lines of various periods as a function of the refractive index change in the dielectric component of the waveguide above it. (For interpretation of the references to colours in this figure legend, the reader is referred to the web version of this paper.)

gest impact. The effect of changing the refractive index for this case is presented in Fig. 2b. We can see that the refractive index change of just 10^{-3} already gives a reasonable change in transmission. The change of the refractive index can be initiated by an external laser pulse or by another control SPP wave. The wavelength of the control SPP wave can be chosen in such a way that the transmission for it can be zero as well, so all its energy will circulate in the ring initiating the refractive index change. Moreover the change in this case will be maximal at the metallic surface, exactly in the region it is most important. Thus an all-SPP active element can be implemented.

3. Bragg reflector

For the active plasmonic device based on the Bragg reflector we chose the geometry which demonstrated the best results as a passive element, particularly a metallic grating placed on the top of the metal [8]. DLSPPW made from a non-linear material is deposed above it (Fig. 3a). The advantage of an active Bragg reflector is that it will be possible to modulate both reflection and transmission of an SPP mode.

The performance of the reflector is a trade-off between the reflecting and scattering power of the grating, both defined by the number of grating lines as well as the grating height. Choosing a compact 10-element grating BR we optimized the grating geometry and found the best grating hight to be $h = 0.06\lambda_{SPP} = 0.06\lambda/n_{eff}$. When the refractive index of the non-linear material is changed by external stimulation, the Bragg condition for the SPP waves is violated and reflection decreases dramatically. The periods of the grating considered here were specially adjusted by an offset from the ideal Bragg period ($P_{Bragg} = \lambda_{SPP}/2 = 601$ nm) to be on the edge of high reflectivity based on the Bragg condition (Fig. 3b), so that small changes of the refractive index provide a dramatic change in reflection and transmission. We have developed a set of active devices on the basis of a Bragg reflector with different grating periods, covering a large range of prospective materials having different possible refractive index changes. The period $P = 665$ nm, being the most distant from the ideal Bragg period requires the smallest change in the refractive index of about $3 \div 5 \times 10^{-3}$ to obtain the required contrast in the reflection (Fig. 3c). On the other hand $P = 655$ nm requires a larger change, however having the advantage of higher overall change. The period $P = 660$ nm, being the compromise between these tendencies seems to be the most beneficial, having the steepest slope in the both reflection and transmission dependences (Fig. 3c and d). Importantly, in all cases the size of the active element is around 5 μm.

4. Conclusions

In conclusion, we have developed a variety of highly-efficient and compact active plasmonics components. In combination with passive waveguiding elements, demonstrated previously both numerically and experimentally, this leads to the realization of highly-integrated information processing photonic circuits on the basis of dielectric-loaded surface plasmon polariton waveguides. Finally, we note that the refractive index change can be induced through thermo-optical or electro-optical effects, leading to thermo-optical and electro-optical active plasmonic components.

Acknowledgments

This work was supported in part by EPSRC (United Kingdom) and EC FP6 STREP PLASMOCOM. The authors acknowledge the fruitful discussions with S.I. Bozhevolnyi.

References

[1] H. Raether, Surface Plasmons on Smooth and Rough Surfaces and Gratings, Springer-Verlag, 1988.
[2] L. Liu, Z. Han, S. He, Opt. Exp. 17 (2005) 6645.
[3] S.A. Maier, P.G. Kik, H.A. Atwater, Appl. Phys. Lett. 81 (2002) 1714.
[4] S.I. Bozhevolnyi, V.S. Volkov, E. Devaux, J.-Y. Laluet, T.W. Ebbesen, Nature 440 (2006) 508.
[5] M. Yan, M. Qui, JOSA B 24 (2007) 2333.
[6] J. Takahara, S. Yamagishi, H. Taki, A. Morioto, T. Kabayashi, Opt. Lett. 22 (1997) 475.
[7] A. Degiron, S.-Y. Cho, C. Harrison, N.M. Jokerst, C. Dellagiacoma, O.J.F. Martin, D.R. Smith, Phys. Rev. A 77 (2008) 475.
[8] A.V. Krasavin, A.V. Zayats, Phys. Rev. B 78 (2008) 045425.
[9] T. Holmgaard, Z. Chen, S.I. Bozhevolnyi, L. Markey, A. Dereux, A.V. Krasavin, A.V. Zayats, Opt. Exp. 16 (2008) 13585.
[10] B. Steinberger, A. Hohenau, H. Ditlbacher, F.R. Aussenegg, A. Leitner, J.R. Krenn, Appl. Phys. Lett. 91 (2007) 081111.
[11] E.D. Palik (Ed.), Handbook of Optical Constants of Solids, Academic Press, New York, 1984.
[12] T. Holmgaard, Z. Chen, S.I. Bozhevolnyi, L. Markey, A. Dereux, A.V. Krasavin, A.V. Zayats, Appl. Phys. Lett. 94 (2009) 051111.
[13] Z. Chen, T. Holmgaard, S.I. Bozhevolnyi, A.V. Krasavin, A.V. Zayats, L. Markey, A. Dereux, Opt. Lett. 34 (2009) 310.
[14] A. Yariv, P. Yeh, Photonics: Optical Electronics in Modern Communications, Oxford University Press, 2007.
[15] A. Yariv, Electron. Lett. 36 (2000) 321.